Particle Accelerators, 1992, Vols. 37–38, pp. 289–299
Reprints available directly from the publisher
Photocopying permitted by license only

BEAM EXPERIMENTS AT COOLER SYNCHROTRON TARN II

TAKESHI KATAYAMA

Institute for Nuclear Study, University of Tokyo 3-2-1, Midoricho, Tanashi, Tokyo 188, Japan.

(Received 3 December 1990)

A cooler synchrotron, TARN II, has been in operation since the beginning of 1989. It aims at an energy of up to 1.1 GeV for protons and 370 MeV/u for heavy ions of $q/A = 0.5$, corresponding to a maximum magnetic rigidity of 5.8 T-m. An electron cooling device and a slow extraction channel have been prepared for various beam experiments. In this paper, the status of TARN II is described, as are the recent results of beam experiments.

1 INTRODUCTION

TARN II is an experimental facility for accelerator studies and atomic and nuclear physics. In addition to the functions of beam acceleration and slow extraction, it is equipped for electron cooling[1]. This cooler synchrotron has a maximum magnetic rigidity of 5.8 T-m, corresponding to a proton energy of 1.1 GeV. The main parameters of the ring are shown in Table 1. The ring is hexagonal, with an average diameter of 24.8 m. Its circumference is 77.76 m, or 17 times the extraction orbit of the injector cyclotron. It has 6 long, straight sections, each 4.2 m. They are used for the beam injection system, an rf cavity, an electron cooling device, and a slow beam-extraction system. It takes 3.5 s for the power supply to fully excite the whole magnet system. The flat-top duration of magnetic field is variable and is long enough for beam cooling and extraction. The rf cavity can be tuned from 0.5 to 8.5 MHz and the power amplifier provides 5 kW, producing a gap voltage of 2 kV. The electron cooling system can cool an ion beam that has an energy of up to 200 MeV/u, corresponding to a maximum electron energy of 120 keV. It consists of an electron gun, an interaction region 1.5 m in length, and collector and electron guiding coils.[2]

The first attempt at beam injection was performed in December 1988, and alpha-particle beams of 28 MeV were circulated in TARN II. Subsequently, experiments in beam accumulation and acceleration have been performed for several days per month, as were the studies of electron cooling. In September 1989, the first cooling experiments were performed successfully with 20-MeV proton beam. Further experiments in beam acceleration and cooling are being performed presently, and are expected to be finished by the end of 1990. After these accelerator studies, TARN II

TABLE 1
Main Parameters of TARN II Ring

Maximum magnetic rigidity	5.8 T.m
Max. beam energy proton	1.1 GeV
ions with $q/A = 1/2$	370 MeV/u
Circumference	77.76 m
Average radius	12.376 m
Radius of curvature	4.045 m
Focusing Structure	FBDBFO
Length of long straight section	4.20 m
Superperiodicity acceleration mode	6
cooling mode	3
Rising time of magnet excitation	3.5 s to full
Repetition rate (max.)	0.1 Hz
Max. field of dipole magnets	15.0 kG
Max. gradient of quadrupole magnets	70 kG/m
Revolution frequency	0.31–3.75 MHz
Acceleration frequency	0.62–7.50 MHz
Harmonic number	2
Max. rf voltage	2 kV
Useful aperture	50×200 mm^2
Vacuum pressure	10^{-11} Torr

will be dedicated to experimental work on nuclear and atomic physics, as well as the interdisciplinary sciences using heavy ion beams.

2 MAGNET SYSTEM

The focusing structure of the magnet system is based on a focusing-defocusing (FODO) lattice, and the long straight sections are provided by inserting a 4.20-m drift space between horizontally focusing quadrupole magnets at every unit cell (Figure 1). The entire ring is composed of six unit cells. For the acceleration mode, these cells are excited identically and the dispersion function and the maximum β_x value can be kept small, around 10 m, which results in the large machine acceptance, 400 π mm-mrad. Horizontal and vertical tune values, Q_x and Q_y, are around 1.75 in this mode. On the other hand, to realize zero dispersion at straight sections for momentum cooling, the superperiodicity is reduced from six to three by changing the excitation current of the quadrupole magnets. In this cooler ring mode, the maximum β_x-value becomes large, around 16 m, and the acceptance is reduced to 140 π mm-mrad.[3] Tunes are $Q_x = 2.25$ and $Q_y = 1.25$, respectively in this operation mode.

The excitation of current for the magnets are performed with four power supplies, one for the dipole magnets and three for the quadrupole magnets. The ramp shape of the dipole field **B** is a trapezoid with a repetition rate of 0.1 Hz and a risetime of 3.5 s. The currents of the three quadrupole-magnet power supplies of Q magnets are tracked, along with the bending-magnet current, within the tracking error of less than 1×10^{-4} with use of the self-teaching procedure in the control computer system.[4]

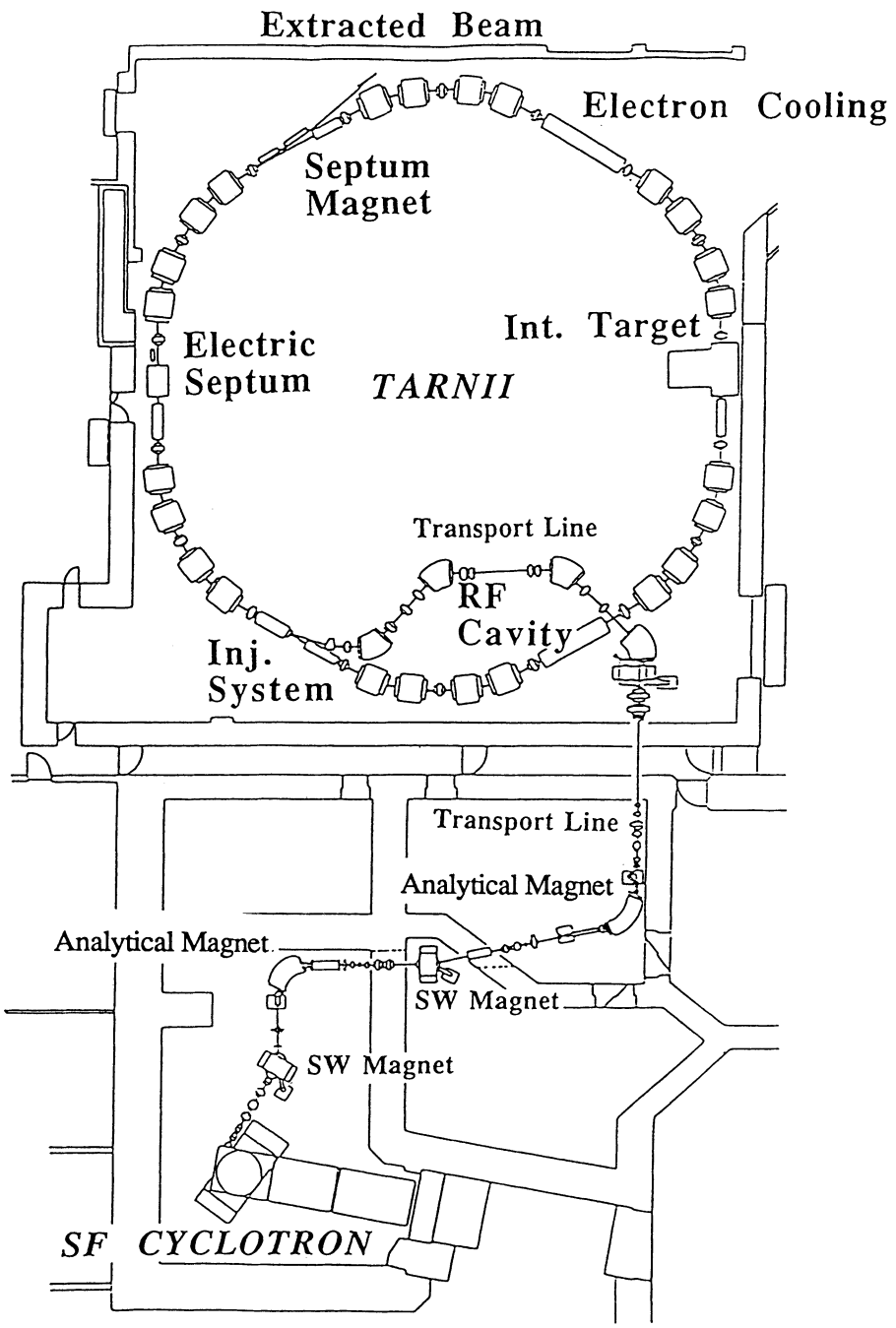

FIGURE 1 Layout of TARN II.

3 VACUUM SYSTEM

A vaccum of better than 10^{-10} Torr is required for the accumulation and acceleration of heavy ion beams, so the vacuum chamber and other elements are free of organic materials. The ramping rate of the magnetic field is as low as 0.45 T/s, so we were able to make the vacuum chambers at the dipole and quadrupole magnets out of 4-mm-thick SUS 316L steel. By sending current flowing directly through the chambers, we can bake them to 250°C. Details of the vacuum system are described in another paper[5]. Presently, the average vacuum pressure in the ring is several times 10^{-10} Torr; and the goal of 10^{-11} Torr will be obtained after the chambers have been baked well.

4 RF SYSTEM

The lowest injection energy was chosen to be 2.58 MeV/u for $^{20}Ne^{4+}$ (among the various ions from the sector-focused cyclotron), corresponding to the revolution frequency of 0.307 MHz in the TARN II ring. At the top energy of 1100 MeV for protons, the revolution frequency is 3.5 MHz; thus the ratio of the lowest to highest frequencies is around 11. The harmonic number was chosen to be 2, and the designed acceleration frequency is 0.6 MHz to 7.0 MHz. An acceleration voltage of 2 kV within the acceleration period of 3.5 s is sufficient for a beam with an 0.5% momentum spread.

The rf cavity is a single-gap, ferrite-loaded, two-quarter-wave coaxial resonator. It covers the frequency range from 0.6 to 8.0 MHz by changing the ferrite bias current from 0 to 770 A. A power amplifier with a maximum output power of 5 kW can produce 2 kV of accelerating voltage throughout the whole frequency range.[6]

The low-level rf electronics system is composed of a voltage-controlled oscillator (VCO) and several feedback loops. Three memory modules store the ramp data: rf frequency, acceleration voltage, and bias current as functions of bending-magnet field strength. At every 1-gauss increment, measured at the 25th dipole magnet, the data are read from memories and converted into analog voltages through digital-to-analog converters (DACs). The data are fed into a VCO, amplitude modulator, and bias current power supply, respectively. The error of bias current or equivalently the degree of cavity detuning, is detected as the phase difference between the rf signals at the grid and the plate of the final power tube. It is used for the correction of resonance frequency of cavity via a hardware feedback loops (AFC). In addition, the signals of horizontal beam position (ΔR) and of the phase error ($\Delta\phi$) between beam bunch and acceleration RF field, are fed back to the voltage controlled oscillator for the correction of RF frequency. The output RF signal of this oscillator is fed to the driver- and power amplifiers.[7]

During the injection period the VCO is phase–locked with the rf signal by using a frequency synthesizer. The frequency and voltage in the injection period are finely adjusted for maximum capture efficiency. In Figure 2, the block diagram of the rf system is shown. Triggering off the master pulse, the excitation of bending- and

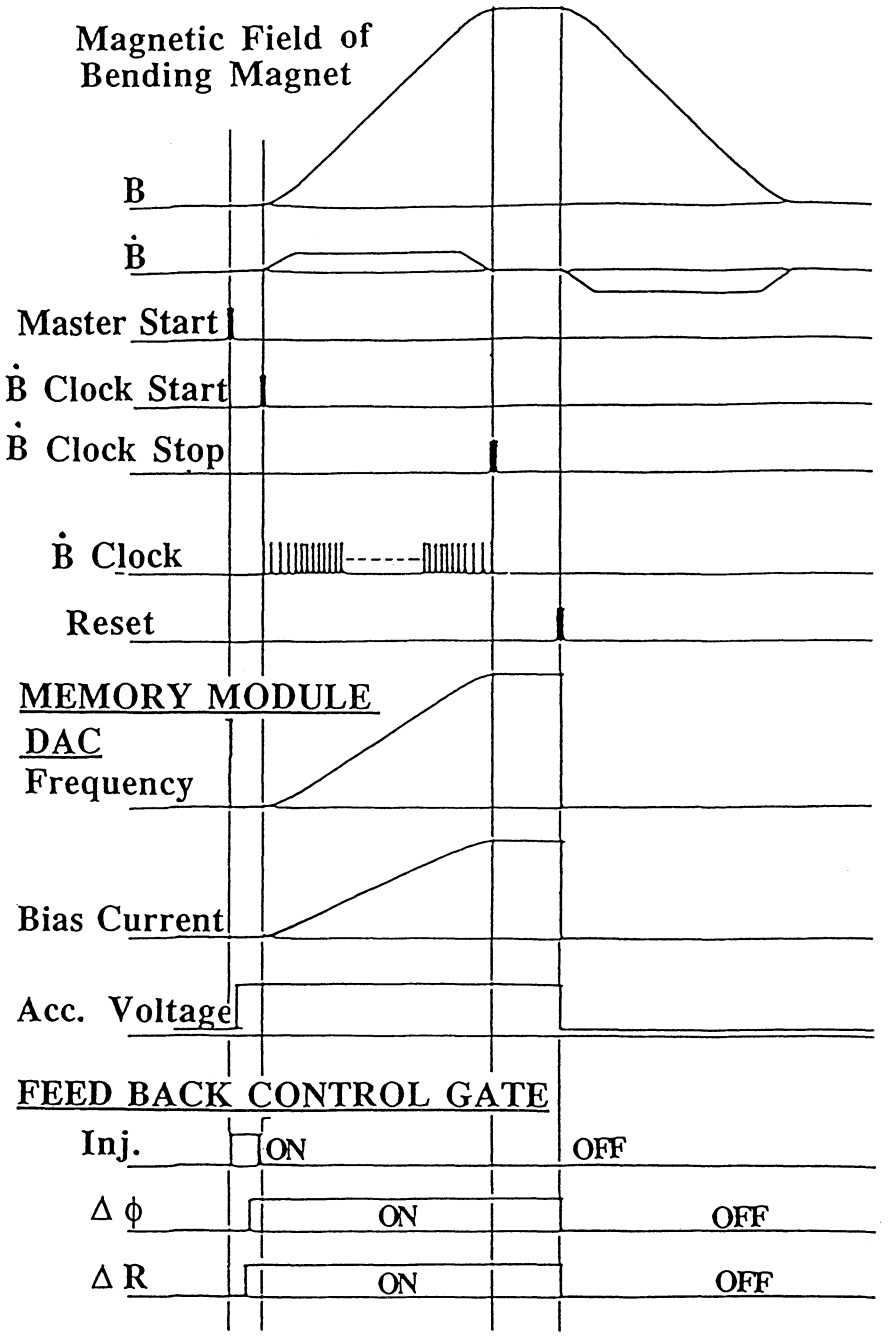

FIGURE 2 Timing chart of rf system. Triggered by the master pulse, the excitation of the magnets and the $d\mathbf{B}/dt$ clock pulse begin. Feedback control gates and other timing signals are provided, with proper delays. A reset pulse restores the data in the memory modules to the initial values.

quadrupole magnets, $d\mathbf{B}/dt$-clock, feedback control gates, and other timing signals, are generated with the proper delays.

5 SLOW BEAM EXTRACTION

The accelerated beams, such as protons, alphas, and Ne, will be slowly extracted from TARN II, for experimental use. The energy range of extraction is from 150 to 350 MeV/u. The extraction scheme is designed to use third-order resonance, and the operation point is moved from the normal ($Q_H = 1.75$, $Q_V = 1.80$) to resonance ($Q_H = 1.6667$, $Q_V = 1.80$) by changing the excitation of the quadrupole magnets. A sextupole magnet is used as an nonlinear field source. The ions whose betatron amplitudes become larger than 75 mm pass into an electrostatic septum, which deflects the ions by 5.8 mrad. The maximum voltage at the electrostatic septum is 80 kV. The thin septum is composed of wires of 90 μm in diameter at 1.25-mm intervals. The effective thickness of the septum wires, seen by the ion beam, is 0.15 mm. The septum magnet is located one sextant downstream from the electrostatic septum, which deflects the ions another 85.2 mrad to extract the ions from the TARN II ring. Presently all the equipment is complete and the studies of beam extraction have started.[8]

6 BEAM EXPERIMENTS

Typical results of experiments on α-beam injection, accumulation and acceleration are as follows. At the exit of the cyclotron, the α-beam energy was 40 MeV and the emittance was measured at 15 π mm-mrad (horizontal) and 20 π mm-mrad (vertical), and the momentum spread was 0.2%. One third of the beam was transported from the exit of the cyclotron to the injection point of TARN II. The beam was multi-turn injected into the ring by two bump magnets excited with a repetition rate of 30 Hz. The decay times of the bump fields were set to approximately 40 μs, which corresponds to about 20 times of the revolution period of the beam in the ring. The frequency of rf field was set to a value corresponding to the harmonic number (2) of the beam circulation: 1.113 MHz for α beams at 40 MeV. Figure 3 shows the signals of the pulsed arc of the ion source in the cyclotron, the discharge currents of the kicker magnet for the beam chopper, and the two bump magnets. Judging from the beam signal of the electrostatic monitor, the gain of intensity of the circulating beam was increased during about 14 turns, which corresponds well with the value expected from the simulations.

The lifetime of the beam was measured by the decay constant of the signal from one of the electrostatic monitors (Figure 4). The e-folding lifetime was found to be 75 s. Beam losses are dominated by scattering off the residual gas. This lifetime is roughly in agreement with the calculated result, subject to the condition that the average vacuum pressure in the ring was about 8×10^{-10} Torr. The tune values were measured, with the rf knockout method, as 1.737 (horizontal) and 1.825 (vertical).

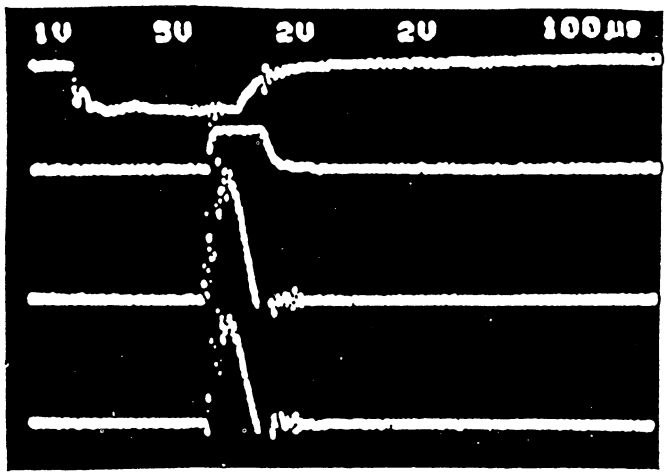

FIGURE 3 Pulse shapes of cyclotron arc, magnetic fields of kicker magnet and two bump magnets (from top to bottom). The bump fields are around 200 G.

The acceleration tests were performed to the top energy of 240 MeV for α particles, which is presently limited by the capacity of the electric power station in the institute. Capacity improvements are under construction, and acceleration to the designed top energy, 370 MeV/u, is expected in December 1991.

In Figure 5, the excitation pattern of the bending magnet and the accelerated beam current are shown. During the acceleration period, beam loss was kept almost negligible with fine adjustment of $\Delta\phi$ with and ΔR feedback-loop gain control in the low-level rf system. The number of accelerated particles was around 10^8. Much

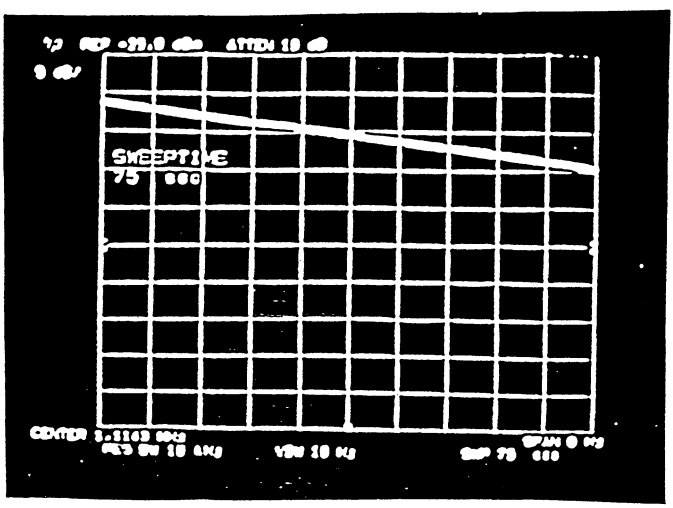

FIGURE 4 Beam signals from the electrostatic monitor (5 dB/div). Horizontal scale is 7 s/div.

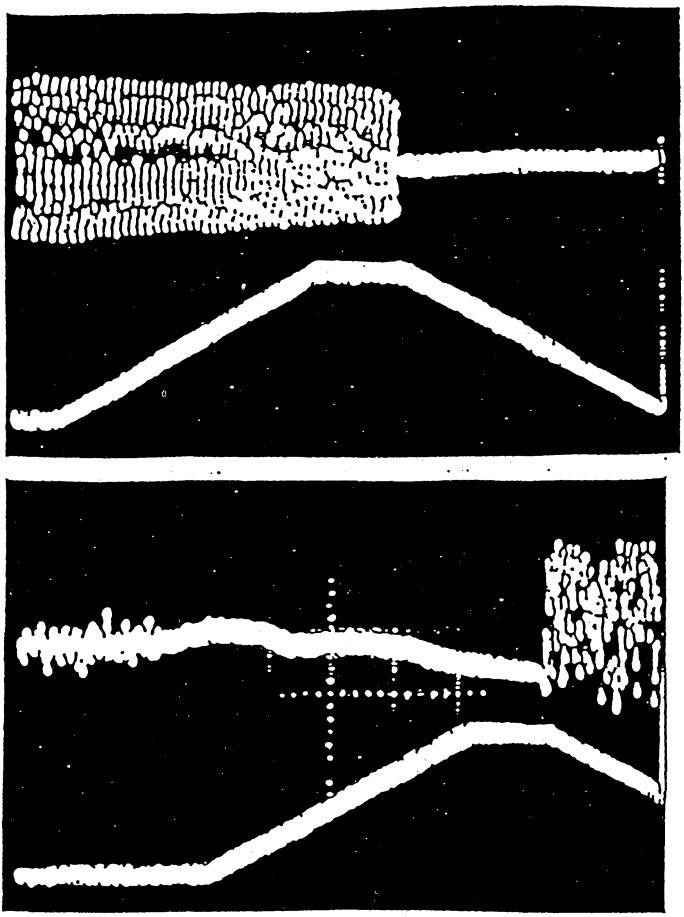

FIGURE 5 Upper: Excitation pattern of the bending magnet (1 s/div) and the intensity of accelerated beam current. Lower: Deviation of the closed orbit (ΔR) during acceleration. Vertical scale is 5 mm/div.

attention was paid to improvement of the sensitivity of the beam monitoring device and to noise reduction of electronic systems. In Figure 5b the detected signal of the beam orbit, ΔR, is shown, and one can see that the deviation of the closed orbit during acceleration was controlled to within several mm.

A strong phase-space compression of the ion beams, to be achieved through electron cooling, will offer new possibilities for accelerator technology and physics research. Since the first success of the electron cooling experiments in September 1989[9], we have continued cooling experiments to examine the details. The electron cooling system is described in Ref 9. The cooling experiments have mainly been performed on a 20 MeV proton beam, which corresponds to an electron energy of 11 keV. A typical electron-beam current is 0.4 A, and the strength of the solenoid field is 600 G. The proton beam was injected into the ring by the multiturn-injection method. The number of injected particles was about 10^7. After adjustment of

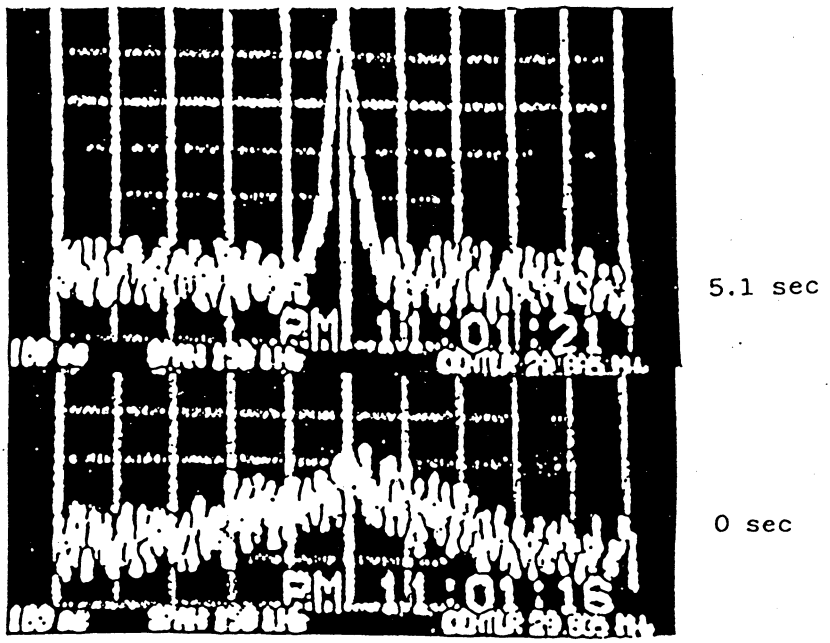

FIGURE 6 Time evolution of momentum spread of a bunched proton beam with cooling. Lower trace: Just after the injection. Upper trace: After 5.1 s. The horizontal scale is 15 kHz/div; the vertical scale is 5 dB/div. The central frequency is 29.985 MHz.

correction magnets, which compensate the effects on the ion beams due to the solenoidal and toroidal magnetic fields of the electron equipment, we observed the cooling effect. The momentum spread of a stored proton beam was improved from the initial value of 2×10^{-3} to the final value of 1×10^{-4} with an e-folding cooling time of several seconds. A typical time evolution of momentum spread (equivalently, the spread of revolution frequency) is given in Figure 6. Machine parameters during electron cooling are given in Table 2.

TABLE 2
Machine Parameters Relevant to Electron Cooling

Proton beam energy	20.26 MeV
Electron beam energy	11.20 keV
Electron current	0.4 A
Initial momentum spread, $\Delta p/p$	2×10^{-3}
Final momentum spread	1×10^{-4}
RF frequency	1.578 MHz
Harmonic number	2
Horizontal β at cooler section	10.2 m
Vertical β at cooler section	3.7 m
Momentum dispersion at cooler section	4.7 m
Horizontal betatron tune	1.71
Vertical betatron tune	1.80

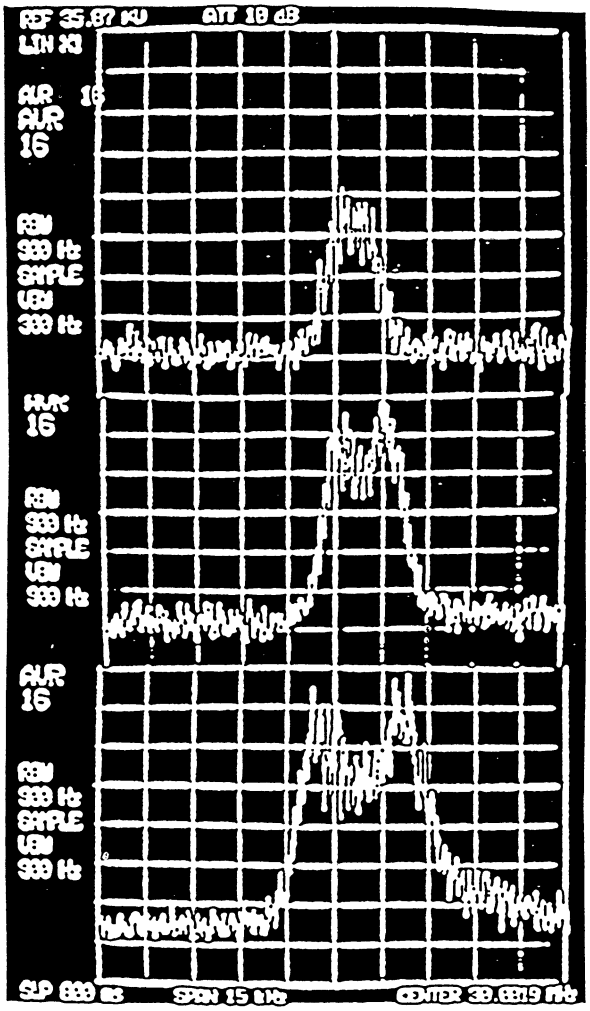

FIGURE 7 Longitudinal Schottky signal spectra. From the top, the numbers of particles in the proton beam are about 3×10^7, 1×10^8, and 3×10^8, respectively.

Several interesting experimental results are obtained on the cooled beams.[10] First, in order to increase the beam intensity, electron cooling was applied during beam injection. The strong phase-space compression due to cooling allows stacking, or repeated multiturn injection. About 20 batches were accumulated, resulting in a stored–beam intensity of 10^8 particles. This cooling-stacking method will be quite useful for accumulating beams of unstable nuclei or rare particles in the storage ring. Second, the Schottky spectra of the coasting proton beams observed by the spectrum analyzer show a two-peak splitting structure within the peak. The splitting increases with the number of stored protons. This phenomenon is known to be caused by collective motion of circulating particles, and the splitting is due to plasma waves,

which rotate with or against the beam direction[12]. Third, a neutral beam is produced when cooling electrons are captured by the circulating proton beam. The neutral beam carries a lot of important information concerning electron– and proton–beam properties. From the horizontal and vertical distributions of neutral atoms, measured at 4.5 m downstream of the cooling section, the beam emittance can be deduced to be 1–2 π mm-mrad, which is much smaller than the initial values, of the order of 100 π mm-mrad.

ACKNOWLEDGEMENT

This work has been done with the collaboration with the TARN II group members at the Institute for Nuclear Study, University of Tokyo.

REFERENCES

1. T. Katayama, in *Proceedings of the 11th International Conference on Cyclotrons and Their Applications* (Ionics, Tokyo, 1986), pp. 128–132.
2. T. Tanabe *et al.*, in *Proceedings of the IEEE Particle Accelerator Conference.*, (Chicago, IL, USA, 1989).
3. A. Noda, in Proceedings IEEE Particle Accelerator Conference. 1987, pp. 846–847.
4. S. Watanabe *et al.*, in *Proceedings of the 7th Symposium on Accelerator Science and Technology* (1990), pp. 249–251.
5. A. Mizobuchi and K. Chida, in *Proceedings of the 19th INS International Symposium on Cooler Rings and their Applications* (Tokyo, 1990).
6. K. Sato *et al.*, in *Proceedings of the 11th International Conference on Cyclotrons and their Applications* (Ionics, Tokyo, 1986), pp. 333–336.
7. T. Katayama *et al.*, in *Proceedings of the 7th Symposium on Accelerator Science and Technology*, 1990, pp. 80–82.
8. A. Noda, Institute for Nuclear Studies report INS-T-498 (1990).
9. T. Tanabe *et al.*, in *Proceedings of the 7th Symposium on Accelerator Science and Technology* (1990) pp. 201–203.
10. T. Tanabe and T. Watanabe, *Nucl. Instrum. Meth. A* **278**, 241 (1989).
11. T. Tanabe, Institute for Nuclear Studies report INS-T-498 (1990).
12. V. V. Parkhomchuk and D. V. Pestsikov, *Sov. Phys. Tech. Phys.* **25**, 7 (1980).